High Resolution Passive THz Imaging Array with Polarization Reusage in 22nm CMOS

van Berkel, S.L.; Malotaux, E.S.; Spirito, M.; Cavallo, D.; Neto, Andrea; Llombart, N.

DOI
10.1109/IRMMW-THz.2019.8874183

Publication date
2019

Document Version
Accepted author manuscript

Published in
2019 44th International Conference on Infrared, Millimeter, and Terahertz Waves (IRMMW-THz)

High Resolution Passive THz Imaging Array with Polarization Reusage in 22nm CMOS

S.L. van Berkel[1], E.S. Malotaux[2], B. van den Bogert[1], M. Spirito[2], D. Cavallo[1], A. Neto[1], and N. Llombart[1]
[1]Delft University of Technology, Department of Microelectronics, Delft, The Netherlands
[2]Electronics Research Laboratory, Department of Microelectronics, Delft University of Technology, Delft, The Netherlands

***Abstract*— A 12-pixel THz Focal Plane Array (FPA), integrated in Global Foundries 22nm CMOS technology, enabling high resolution passive THz imaging, is presented. The array efficiently couples blackbody radiation from 200 GHz to 600 GHz to Schottky Barrier Diodes (SBDs) in a differential topology. An antenna-detector co-design results in an average Noise Equivalent Power (NEP) of 0.9 pW/$\sqrt{\text{Hz}}$. An extremely small array periodicity is achieved by using two orthogonal polarizations. Such configuration enables passive imaging with a near-diffraction limited resolution while simultaneously maintaining a high optical efficiency of 42%. The array is currently in tape-out and measurements will be presented at the conference.**

I. Introduction and Background

Uncooled THz imagers often rely on active sources to generate an image [1,2]. To realize real-time THz radiometry (i.e. imaging without active sources), a large portion of the THz-spectrum should efficiently be exploited [3] together with an antenna-detector co-design to maximize the power transfer between the antenna and detector. Efficient and wideband operation of CMOS integrated antennas has been demonstrated in IRMMW-THz 2018 [4] where gain and radiation patterns measurements of a double-bow tie slot antenna, operating from 200 GHz to 600 GHz were presented, in excellent agreement with simulations. A subsequent step in going to a multi-pixel FPA, brings in more challenges in terms of sampling efficiency and resolution (i.e. beam separation of adjacent pixels) of the imaging system [3]. A high resolution can only be achieved when the array periodicity is extremely small, directly compromising the efficiency of the antenna. Tightly sampled arrays suffer from high mutual coupling between adjacent pixels and less directive antenna feeds that illuminate a dielectric lens poorly. A viable antenna solution to design efficient, wideband, tightly sampled FPAs is by resorting to a connected array architecture [5]. The leaky-wave supported by the architecture results in an increased directivity of the array elements, drastically increasing the illumination efficiency of a dielectric lens [6].

This work presents a wideband passive imaging array, operating from 200 GHz to 600 GHz, achieving high resolution and efficiency by exploiting two polarizations. The passive camera consists of a 22nm CMOS connected array of dipoles, glued to an elliptical silicon lens, that couple the blackbody radiation to SBDs, which are co-designed to optimize NEP and matching efficiency.

II. Imaging System and Detector Architecture

A connected array of dipoles is optimized in Global Foundries 22nm CMOS technology and is shown in Fig. 1(a). The array consists out of 12 pixels. The connected array of dipoles is optimized in transmission, radiating into infinite

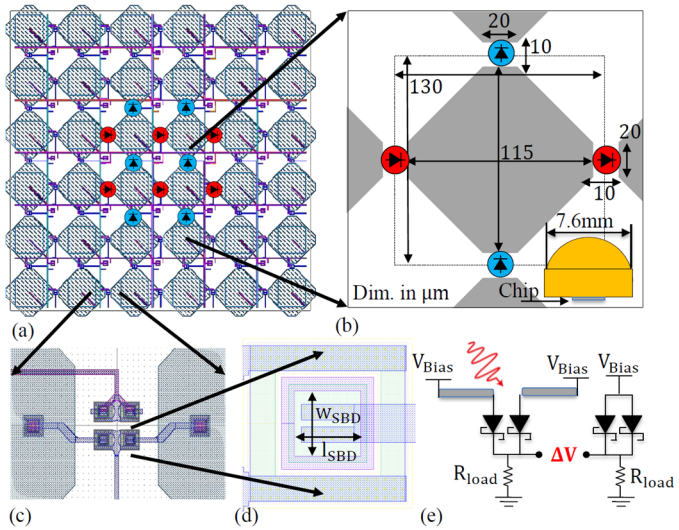

Fig. 1. Connected array architecture. In (a,b) the complete array and dimensions of the unit cell are shown. Subfigures (c-e) illustrate the pseudo-differential read-out using Schottky Barrier Diodes as incoherent detectors.

silicon, by using CST Microwave Studio. The low-resistive silicon of the chip is thinned down to 200 µm to reduce ohmic dissipation. In order for the array to have imaging capabilities, the chip is glued to an elliptical silicon lens with diameter D = 7.6 mm, such that the incident radiation is focused on the individual pixels. To reduce the reflections between the silicon-air interface, the elliptical the lens is provided with a Parylene C anti-reflection coating. The dipoles of the array are tapered with a 45° degree angle. Tapering the dipoles reduces the mutual coupling between the pixel elements. Furthermore the array becomes geometrically identical in both the horizontal and vertical polarization directions. Such antenna architecture allows for doubling the amount of pixels, by exploiting both polarizations on the same chip area. Since the two polarizations are highly decoupled, the angular resolution is doubled without increasing in mutual coupling between the pixels.

A differential read-out topology using SBDs, Fig. 1(c-e), is optimized together with the antenna. A differential symmetry introduces a RF-ground allowing to connect the read-out network without any incident RF-power dissipation losses in the read-out network, that would result in a loss in responsivity of the diodes. The diode responsivity describes the incremental DC-current proportional to the absorption of the blackbody radiation that is coupled from the antenna to the diodes. The loading resistor R_{load} converts this change in DC-current to a change in DC-voltage over the resistor, ΔV, which can be directly read-out, pseudo-differentially, Fig. 1(c,e). The dimensions of the SBDs, w_{SBD} and l_{SBD}, and loading resistor R_{load} are iteratively optimized using the optimization function

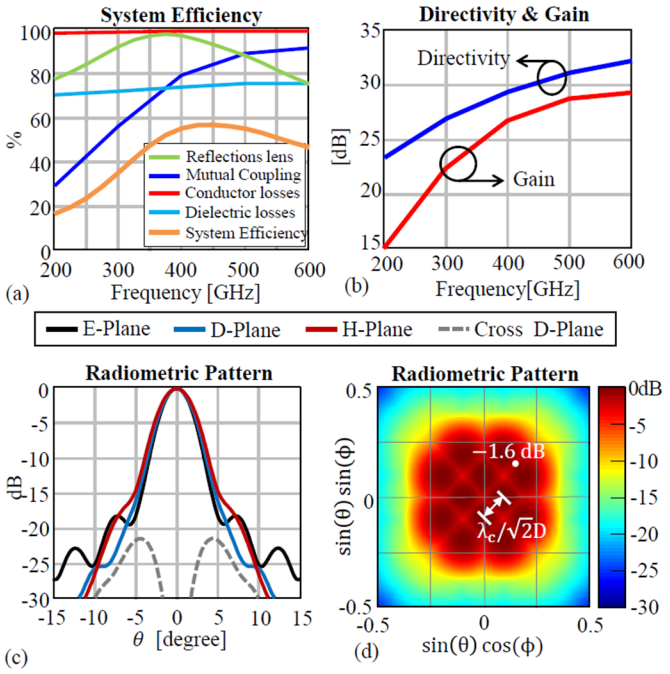

Fig. 2. Performance of the quasi-optical system. In (a) the system efficiency is shown, leading to a system gain shown in (b). The gain patterns, integrated over frequency, i.e. the radiometric pattern, is shown in (c) for a single pixel whereas (d) shows the complete Field-of-View of the array.

$\mathrm{OptFunc}(w_{SBD}, l_{SBD}, R_{load}) = \frac{1}{\Delta f_{RF}} \int_{\Delta f_{RF}} \frac{\mathrm{NEP}(f)}{\eta_\Omega(f)} \mathrm{d}f$, where $\eta_\Omega(f)$ is the impedance matching efficiency of the detector-antenna combination. The high capacitive input impedance of the SBDs requires an iterative co-design to conjugately match the input impedance of the antenna. An inductive impedance is realized with the placement of the vias that connect the dipoles to the SBDs.

RADIOMETRIC PERFORMANCE

The dimensions of the optimized array, in μm, are shown in Fig. 1(b) for the unit cell. The efficiency of the complete system is shown in Fig. 2(a). The main contributions to the system efficiency are the dielectric losses in the low-resistive silicon and mutual coupling between the pixels, inherent to tightly sampled arrays. The ohmic loss could be reduced further by further thinning down the CMOS wafers. The radiometer has a high average system efficiency of 42% over the full bandwidth, despite the tight sampling. The directivity and gain of the imaging system are shown in Fig. 2(b). In radiometry, since the radiometer integrates power incoherently over the full bandwidth and no spectral information can be resolved in the output signal, a suitable way to evaluate the imaging performance of the quasi-optical system is by calculating its effective radiometric pattern, as defined in [3]. The 1D-cuts of the radiometric pattern of a single element and the 2D-plot of the radiometric pattern of the complete array are shown in Fig. 2(c) and (d) respectively. The effective radiometric pattern is clean and symmetric and the cross-polarization is lower than -20 dB. The roll-off between beams of adjacent pixels is just -1.6 dB and the resolution in the diagonal planes is $\Delta\theta = \lambda/\sqrt{2}D$, achieving a nearly diffraction limited camera (i.e. when $\Delta\theta = \lambda/2D$ [3]).

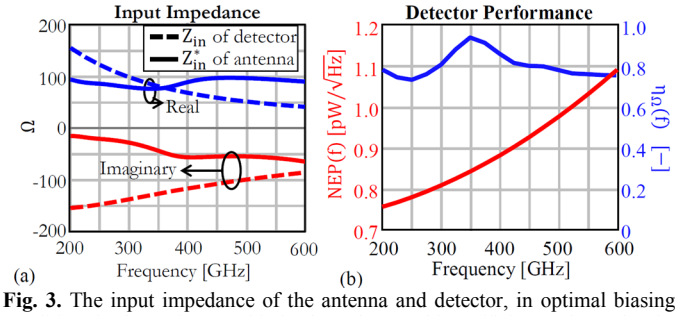

Fig. 3. The input impedance of the antenna and detector, in optimal biasing condition, is shown in (a). This leads to the matching efficiency shown by the blue line and scale in (b). The NEP of the detector is shown in red.

After an iterative co-design of the antenna and detector, by using the optimization function introduced in the previous section, the dimensions of the optimized SBDs are $w_{SBD} = l_{SBD} = 1.6$ µm and $R_{load} = 2$ kΩ. Fig. 3(a). shows the input impedance of both the antenna and detector (at optimum biasing voltage). The highly capacitive behavior of the detector can only partly be compensated with the inductive behavior of the antenna, leading to an impedance matching efficiency of approximately ~85% as shown in Fig. 3(b). The system requires modulation of the signal in order to avoid high flicker-noise contributions that are introduced by the detector. In the white noise region of the detector, the NEP is simulated as shown by the red curve in Fig. 3(b).

CONCLUSIONS

The temperature sensitivity of a radiometer represents the minimum temperature difference in the object of interest that one can resolve from noise fluctuations in the image. With an average NEP of 0.9 $\mathrm{pW}/\sqrt{\mathrm{Hz}}$, together with an average system efficiency of 42%, a sub-Kelvin temperature sensitivity can be achieved without having to resort to the use of active sources [3], enabling low-cost imaging applications in the THz regime. The array is currently in tape-out and the diodes are being characterized. The measurements will be presented during the conference.

ACKNOWLEDGEMENTS

This research is supported by the Dutch Technology Foundation STW (TiCAM, 13325), which is part of the Netherlands Organization for Scientific Research (NWO), and which is partly funded by the Ministry of Economic Affairs. N. Llombart would like to thank the European Research Council for the starting grant LAA-THz-CC (639749).

REFERENCES

[1] R. Hadi et. al., "A 1 k-Pixel Video Camera for 0.7-1.1 Terahertz Imaging Applications in 65-nm CMOS", *IEEE J. Solid-State Circuits*, Dec. 2012.
[2] G. C. Trichopoulos, et.al., "A Broadband Focal Plane Array Camera for Real-time THz Imaging Applications," IEEE TAP, 2013.
[3] S. L. van Berkel, et. al., "THz imaging using uncooled wideband direct detection focal plane arrays," *IEEE Trans. THz Sci. Technol.*, Sep. 2017.
[4] S. L. van Berkel, et. al., "Optical Performance of a Wideband 28nm CMOS Double Bow-Tie Slot Antenna for Imaging Applications," *IRMMW-THz 2018*.
[5] D. Cavallo and A. Neto, "A connected array of slots supporting broadband leaky waves," IEEE TAP, vol. 61, no. 4, pp. 1986–1994, 2013.
[6] A. Neto, "UWB, Non Dispersive Radiation from the Planarly Fed Leaky Lens Antenna - Part 1: Theory and design," IEEE TAP, 2010.